

Impossible moons - Transit timing effects that cannot be due to an exomoon

David Kipping^{1,2*} and Alex Teachey¹

¹*Dept. of Astronomy, Columbia University, 550 W 120th Street, New York NY 10027*

²*Center for Computational Astrophysics, Flatiron Institute, 162 5th Av., New York, NY 10010*

Accepted . Received ; in original form

ABSTRACT

Exomoons are predicted to produce transit timing variations (TTVs) upon their host planet. Unfortunately, so are many other astrophysical phenomena - most notably other planets in the system. In this work, an argument of *reductio ad absurdum* is invoked, by deriving the transit timing effects that are impossible for a single exomoon to produce. Our work derives three key analytic tests. First, one may exploit the fact that a TTV signal from an exomoon should be accompanied by transit duration variations (TDVs), and that one can derive a TDV floor as a minimum expected level of variability. Cases for which the TDV upper limit is below this floor can thus be killed as exomoon candidates. Second, formulae are provided for estimating whether moons are expected to be “killable” when no TDVs presently exist, thus enabling the community to estimate whether it’s even worth deriving TDVs in the first place. Third, a TTV ceiling is derived, above which exomoons should never be able to produce TTV amplitudes. These tools are applied to a catalog of TTVs and TDVs for two and half thousand *Kepler* Objects Interest, revealing over two hundred cases that cannot be due to a moon. These tests are also applied to the exomoon candidate Kepler-1625b i, which comfortably passes the criteria. These simple analytic results should provide a means of rapidly rejecting putative exomoons and streamlining the search for satellites.

Key words: planets and satellites: detection — planets and satellites: individual (Kepler-1625b) — methods: analytical

1 INTRODUCTION

Transit timing variations (TTVs) have long been recognized as a powerful tool for the detection of exoplanets (Dobrovolskis & Borucki 1996a,b; Miralda-Escudé 2002; Schneider 2003, 2004; Holman & Murray 2005; Agol et al. 2005), as well as exomoons (Sartoretti & Schneider 1999; Szabó et al. 2006; Simon et al. 2007; Kipping 2009a,b). Early searches for TTVs, largely focussing on hot-Jupiters, were characterized by either null detections (Steffen & Agol 2005; Miller-Ricci et al. 2008a,b; Rabus et al. 2009; Hrudková et al. 2010) or signals that later turned out to be spurious (Díaz et al. 2008; Ribas et al. 2009; Maciejewski et al. 2010) - so much so that one could be forgiven for questioning the value of the TTV enterprise at the time.

This situation radically changed though with the launch of *Kepler* (Holman & Murray 2005; Ballard et al. 2011; Nesvorný et al. 2013; Holzer et al. 2016; Hadden & Lithwick 2017) - thanks to its detections of longer period planets and continuous, long-baseline photometric observations.

There are now hundreds of known TTV systems, and this embarrassment of riches has actually presented a problem. Specifically, TTVs due to planet-planet interactions are so common that the search for exomoons is greatly frustrated by this enormous background signal. In this era of abundant TTVs detections, there is a need for tools that can quickly classify what TTVs can/cannot be - an era of TTV triage.

In recent years, much of the theoretical work on TTVs has focussed on the inverse problem (Nesvorný & Morbidelli 2008; Nesvorný & Beaugé 2010; Lithwick et al. 2012; Nesvorný & Vokrouhlický 2014; Deck & Agol 2016). Yet these efforts broadly assume a specific model already - namely that the observed TTVs are caused by another planet. A Bayesian would describe this as parameter estimation. But parameter estimation is only one side of the coin when it comes to inference, with the other being model selection. Certainly, there are many cases where the model can be safely assumed to be that of planet-planet interactions, for example because of the known existence of near mean motion resonance transiting planets (Wu & Lithwick 2013; Hadden & Lithwick 2014, 2017). But it would be folly to assume that all TTVs will be universally caused by planet-

* E-mail: dkipping@astro.columbia.edu

planet interactions - other models should be considered too. And this is of course highly salient for exomoons, which represent a distinct origin of TTVs.

Model selection for TTVs will be particularly challenging when the TTVs are nearly sinusoidal, which is the form taken by circular orbit exomoons¹ (Kipping 2009a). This is because planet-planet interactions are perfectly capable of appearing as sinusoidal, too, for example due to the circulating line of conjunctions (Lithwick et al. 2012; Nesvorný & Vokrouhlický 2014; Deck & Agol 2016). Thus, the waveform shape of the TTVs will not necessarily be useful in distinguishing these two hypotheses. In this work, using just the amplitude of the observed transit timing effects, it is investigated whether this has any ability to test the moon hypothesis. In particular, almost the opposite problem is considered through an argument *reductio ad absurdum* - what kind of transit timing effects can one classify as being impossible for an exomoon?

2 KILLING MOONS BELOW A TDV FLOOR

2.1 Conceptual explanation

Before diving into the mathematical details of the effect described in this section, it is instructive to first offer a simple intuitive explanation to guide what follows. The TTV amplitude of an exomoon is proportional to the mass of the satellite, M_S , multiplied by its semi-major axis, a_S (Sartoretti & Schneider 1999). Consider that one has detected a TTV signal for an exoplanet - a rather typical situation given that there are now hundreds of such planets (Holczer et al. 2016). The task is now to determine if this data in hand is consistent with an exomoon hypothesis, or not.

Consider that there exists an additional piece of information - measurements of the TDVs. Exomoons are predicted to produce TDVs with the same periodicity as the TTV signal, with the dominant TDV component being proportional to $M_S a_S^{-1/2}$ (Kipping 2009a,b). There are far fewer examples of known TDV systems (see Szabó et al. 2012 and Nesvorný et al. 2013 for rare examples) and so let's consider the more typical case that a detected TTV signal does not appear to be accompanied by a TDV signal.

This lack of a clear TDV signal can be translated into a TDV amplitude upper limit, and that limit in fact places some interesting constraints on our problem. For example, a moon in a compact orbit around its planet should produce quite large TDVs, since the amplitude is proportional to $a_S^{-1/2}$. Thus, one should expect that the lack of a TDV detection excludes these inner orbits and places some limit on the minimum orbital radius of the hypothesized exomoon. If the TDV upper limit is sufficiently tight, this minimum or-

bit radius may in fact exceed the Hill sphere² - this would be an *impossible moon*.

Thus, in what follows, the extent to which an exoplanet with a detected TTV amplitude and a TDV upper limit can be used to deduce an minimum allowed exomoon semi-major axis is investigated. If this semi-major axis exceeds the Hill radius, then such cases could thus be dismissed as exomoon candidates, despite the fact only a TTV signal was ever recovered.

2.2 Mathematical details

Let us begin by considering the ratio of the TDV amplitude to the TTV amplitude as caused by an exomoon, denoted by the symbol η . This was first derived in Kipping (2009a), who considered only velocity-induced TDVs (TDV-V). The result is that $\eta = n_S T$, where n_S is the mean motion of the moon ($= 2\pi/P_S$) and T is the planet's transit duration. The power of this equation is that if both effects are detected, the orbital period of the moon can be uniquely inferred, something usually not possible with exomoons due to aliasing effects (Kipping 2009a).

However, $\eta = n_S T$ is only true in the limiting case of i) no transit impact parameter induced TDVs (TDV-TIP), caused by planets bobbing up and down against the planet's orbital plane (Kipping 2009b) ii) zero eccentricity for the satellite. Relaxing both of these assumptions, the ratio of the root mean square (RMS) amplitudes is shown in Kipping (2011) to be given by (see their Equation 6.100), which is written here as

$$\eta = T n_S \underbrace{\frac{1}{(1-e_S^2)^{3/2}} \sqrt{\frac{\Phi_{\text{TDV-V}}}{\Phi_{\text{TTV}}}}}_{\equiv \zeta} + \varepsilon, \quad (1)$$

where $\Phi_{\text{TDV-V}}$ and Φ_{TTV} are scalars controlling the strength of the TDV-V and TTV effects respectively (which depend on the three-dimensional geometry of the orbits), ε is a parameter introduced here to absorb the TDV-TIP component of the η parameter (see Equation 6.100 of Kipping 2011 for full form).

Given that the above is a generalization to eccentric satellite orbits, it is not surprising that the ζ term defined in Equation (1) tends to unity in the limit of $e_S \rightarrow 0$, which is evident from the behaviour of the $(1-e_S^2)^{-3/2}$ term, as well as the fact that

$$\lim_{e_S \rightarrow 0} \Phi_{\text{TTV}} = \lim_{e_S \rightarrow 0} \Phi_{\text{TDV-V}} = \pi(1 - \cos^2 i_S \sin^2 \varpi_S), \quad (2)$$

as shown in Equations (6.47) & (6.67) of Kipping (2011). Although ζ tends towards unity for circular moons, one might wonder whether it is typically greater than unity (i.e. an enhancement factor to η) or less than unity (i.e. an attenuation factor) for $e_S > 0$. Since the functional forms of the Φ_{TTV} and $\Phi_{\text{TDV-V}}$ are rather protracted, it is not straight-forward to analytically investigate this behaviour.

¹ We highlight that this can be somewhat modified for very large moons that distort the transit profile (Simon et al. 2007), but observational constraints on the exomoon population of *Kepler* planets shows that this would be a rare occurrence (Teachey et al. 2018).

² One might question whether quasi-moons outside of the Hill sphere defy this definition, but in this work we consider that quasi-moon are exactly that - "quasi-moons" and not "moons".

Instead, a large number (10^7) of random examples of $0 \leq e_S < 1$, $0 \leq \omega_S < 2\pi$, $0 \leq \varpi_S < 2\pi$ and $0 \leq i_S < 2\pi$ were generated, with a corresponding calculation of ζ . From this, it is found that $\zeta \geq 1$ in every single numerical test, showing that it can only ever serve as an enhancement factor. Generally, one does not expect moons to possess large eccentricities due to tidal circularization, but the following argument holds even in such a case.

Next, consider the behaviour of ε , which relates to the TDV-TIP effect. The TDV-TIP effect is offset in phase from the TDV-V effect by $\pm\pi/2$ radians (depending on whether the moon is prograde or retrograde; see Kipping 2009b). For this reason, it can never destructively interfere with the TDV-V effect to attenuate the signal. Rather, whatever the amplitude of the TDV-TIP effect, and whether it be prograde or retrograde, it can only act to increase the overall TDV amplitude. Thus, $\varepsilon > 0$ in all cases. Therefore, like the ζ term, ε can only act as an enhancement factor to η . Generally, the TDV-TIP effect is small compared to the TDV-V effect (Kipping 2009b), but this is not actually a requisite in the following argument. To summarize the results so far, it has been shown that

$$\eta = \frac{\delta_{\text{TDV}}}{\delta_{\text{TTV}}} = \zeta T n_S + \varepsilon, \quad (3)$$

where δ_{TTV} and δ_{TDV} are TTV and TDV RMS amplitudes (respectively), T is the transit duration, n_S is the satellite's mean motion, and ζ and ε are scalars such that $\zeta \geq 1$ and $\varepsilon > 0$.

With these points established, one may now consider how η can be used to identify impossible moons. Let us replace P_S with P_P using Equation (12) of Kipping (2009a), which establishes that $P_S \simeq P_P \sqrt{f^3/3}$, yielding

$$\frac{\delta_{\text{TDV}}}{\delta_{\text{TTV}}} = \zeta \left(\frac{2\pi\sqrt{3}T}{P_P f^{3/2}} \right) + \varepsilon, \quad (4)$$

where f is the semi-major axis of the moon relative to the Hill radius of the planet (and thus one expects $f < 1$). Consider that one has an upper limit on δ_{TDV} given by $\delta_{\text{TDV,max}}$, such that $\delta_{\text{TDV}} \leq \delta_{\text{TDV,max}}$. Substituting this into our η relation gives

$$\frac{\delta_{\text{TDV,max}}}{\delta_{\text{TTV}}} \geq \zeta \left(\frac{2\pi\sqrt{3}T}{P_P f^{3/2}} \right) + \varepsilon. \quad (5)$$

Since the LHS of the equation is always greater than the RHS, then the inequality will also be true in the case of $\varepsilon \rightarrow 0$ and $\zeta \rightarrow 1$, since these limits represent the smallest allowed values for these terms. Accordingly, one may write - without any loss of generality - that

$$\frac{\delta_{\text{TDV,max}}}{\delta_{\text{TTV}}} \geq \frac{2\pi\sqrt{3}T}{P_P f^{3/2}}. \quad (6)$$

In the above, essentially all terms are observable under the stated assumptions of the problem - except for f . One may thus re-arrange to make f the subject:

$$f^{3/2} \geq \left(\frac{2\pi\sqrt{3}T}{P_P} \right) \left(\frac{\delta_{\text{TTV}}}{\delta_{\text{TDV,max}}} \right). \quad (7)$$

Finally, one can see that the above represents a lower limit on f , denoted as f_{min} , and given by

$$f_{\text{min}} = \left(\frac{2\pi\sqrt{3}T}{P_P} \right)^{2/3} \left(\frac{\delta_{\text{TTV}}}{\delta_{\text{TDV,max}}} \right)^{2/3}. \quad (8)$$

Figure 1 shows some example calculations of f_{min} for an ensemble of KOIs (*Kepler* Objects of Interest) with available TDVs (taken from Holczer et al. 2016), with the data methods described later in Section 5.

Since a moon should always have $f < 1$ (Domingos et al. 2006), one can write a simple criterion that a real exomoon should satisfy:

$$\left(\frac{2\pi\sqrt{3}T}{P_P} \right)^{2/3} \left(\frac{\delta_{\text{TTV}}}{\delta_{\text{TDV,max}}} \right)^{2/3} < 1, \quad (9)$$

or more succinctly, one can define a “TDV floor” criterion is

$$\delta_{\text{TDV,max}} > 2\pi\sqrt{3} \left(\frac{T\delta_{\text{TTV}}}{P_P} \right). \quad (10)$$

To illustrate this, consider the case where the TDV limits are very noisy, such that $\delta_{\text{TDV,max}}$ is poorly constrained, with a very large upper limit. In such a case, the criterion is satisfied. This does not prove the solution is an exomoon, but it means that the current observational constraints are at least consistent with said hypothesis. Now imagine observers obtaining ever more precise TDVs, yet still no significant detection ever emerges, thus gradually lowering $\delta_{\text{TDV,max}}$. Eventually, the criterion will fail and at that point one can confidently assert that the observations are inconsistent with being caused by a single large exomoon - an impossible moon.

3 THE KILLING REGIME

If TDV measurements are expected to be very noisy or too few in number, one might be able to immediately conclude that it's not even worth the effort of attempting to derive TDVs to test the criterion of Equation (10). The fundamental noise limit itself will not be sensitive enough to infer an impossible moon. This is certainly a worthwhile point to consider because TDVs can be computationally expensive to derive. In what follows then, the expected upper limit on the TDV amplitude is derived under some simplifying assumptions.

Consider a sequence of N homoscedastic TDVs with normally distributed noise of standard deviation Δ_{TDV} . Generally, moons are expected to be near circular, producing sinusoidal TDVs Kipping (2009a). It is here assumed that the TDVs are dominated by a single component to simplify the analysis, which will typically be the TDV-V effect (except for grazing transiting planets or highly inclined moons; Kipping 2009b). Accordingly, the model being regressed to the data is

$$\text{TDV}(E) = A_{\text{TDV}} \sin(nE + \phi), \quad (11)$$

where E is the epoch number, ϕ is a phase term and

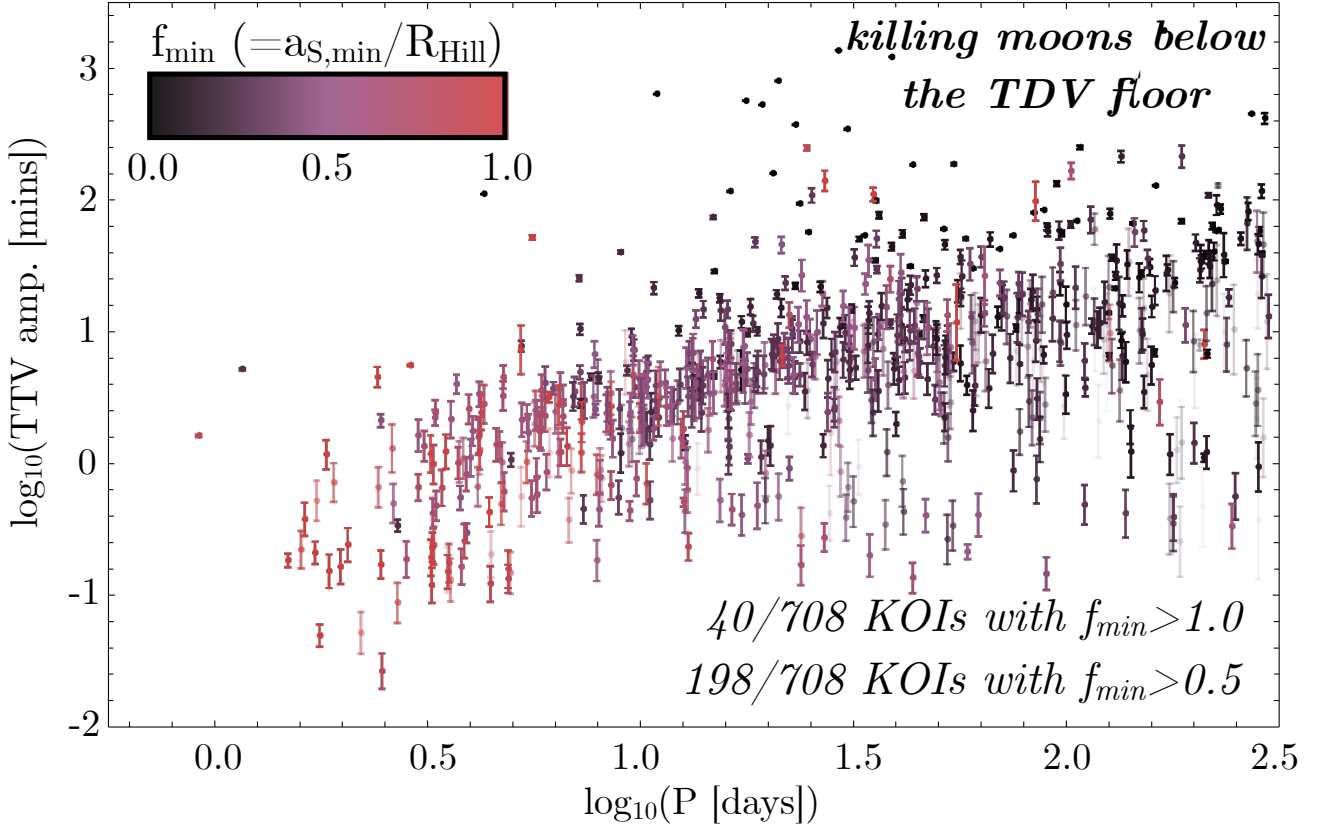


Figure 1. Best-fitting TTV amplitude from a LS periodogram applied to the outlier-cleaned [Holczer et al. \(2016\)](#) TTV catalog, as a function of planetary period. Point opacity equals the $\Delta BIC/10$ score of the fits. The color coding shows the minimum allowed exomoon semi-major axis (given by Equation 8), assuming that the TTVs are caused by a single satellite and conditioned upon the fact no TDVs are observed. 40 KOIs are identified that require $f > 1$ and can thus be killed as exomoon candidates.

n is the TDV frequency. The killing criterion described in Section 2 is for the case where a strong TTV has already been detected. If the signal is due to an exomoon, then the TDVs will have the same periodicity as the TTVs, and that period is presumably well-constrained thanks to the TTV detection. Further, the phase is also known, since TDV-Vs lag TTVs by $\pi/2$ radians ([Kipping 2009a](#)). Accordingly, the only free parameter is the amplitude, which is closely related to the RMS amplitude via $A_{TDV} = \sqrt{2}\delta_{TDV}$.

Since the data are assumed to be normally distributed, and the problem is linear with respect to the one unknown parameter, then one may employ linear least squares regression theory to write that the parameter covariance matrix (a one-by-one matrix in this case) will be given by

$$\Sigma = \Delta_{TDV}^2 (\mathbf{X}^T \mathbf{X})^{-1}, \quad (12)$$

where the homoscedasticity of the problem has been exploited, and \mathbf{X} is given by

$$\mathbf{X} = \begin{bmatrix} \sin(nE_1 + \phi) \\ \sin(nE_2 + \phi) \\ \dots \\ \sin(nE_N + \phi) \end{bmatrix}. \quad (13)$$

Evaluating, one may show that

$$\Sigma = \frac{\Delta_{TDV}^2}{\sum_{i=1}^N \sin^2(nE_i + \phi)}, \quad (14)$$

and thus the error on A_{TDV} will be

$$\sigma_{A_{TDV}} = \frac{\Delta_{TDV}}{\sqrt{\sum_{i=1}^N \sin^2(nE_i + \phi)}}. \quad (15)$$

Sampling of the TDV curve is random, there is no preference for any particular phase to be observed. This means that Σ will not always return the same covariance matrix even for the same number of points with the same uncertainty - the term is probabilistic. It is therefore necessary to estimate the expectation value of Σ accounting for this feature.

One can write that $\sin^2(nE_i + \phi) \rightarrow \sin^2(x_i)$, where x_i is a uniform random variate between 0 and 2π . The probability distribution of $\sin^2 x_i$ is now well-posed, and described by the arc-sine distribution such that

$$\Pr(y_i = \sin^2 x_i) dy_i = \frac{1}{\pi \sqrt{y_i} \sqrt{1 - y_i}} dy_i. \quad (16)$$

The expectation value of the TDV uncertainty now becomes

$$\frac{E[\sigma_{\text{ATDV}}]}{\Delta_{\text{TDV}}} = E\left[\frac{1}{\sqrt{\sum_{i=1}^N y_i}}\right]. \quad (17)$$

In the case of $N \gg 1$, the expectation value of the RHS becomes $2/\sqrt{N}$, such that

$$\begin{aligned} \lim_{N \gg 1} E[\sigma_{\text{ATDV}}] &= \frac{2\Delta_{\text{TDV}}}{\sqrt{N}}, \\ \lim_{N \gg 1} E[\sigma_{\delta_{\text{TDV}}}] &= \frac{\sqrt{2}\Delta_{\text{TDV}}}{\sqrt{N}}. \end{aligned} \quad (18)$$

The upper limit on the TDV amplitude can be expressed as some factor of this noise estimate, with a typical choice being 3. Accordingly, it is estimated that a null TDV signal will have an upper limit of

$$\delta_{\text{TDV,max}} \simeq 3 \times \frac{\Delta_{\text{TTV}}}{\sqrt{2N}}, \quad (19)$$

where the replacement $\Delta_{\text{TDV}} \simeq 2\Delta_{\text{TTV}}$ has also been used - i.e. the duration error is approximately twice the timing error (Carter et al. 2008). This replacement is necessary since the assumption throughout is that the TDVs have not yet been derived and one is deciding as to whether it's worth inferring them. Combining this with our earlier Equation (10) yields the following requirement for an physical exomoon - assuming a TTV signal has been detected and a TDV upper limit:

$$\left(\frac{\delta_{\text{TTV}}}{\sqrt{2}\Delta_{\text{TTV}}/\sqrt{N}}\right) < \left(\frac{\sqrt{3}}{4\pi}\right)\left(\frac{P_P}{T}\right). \quad (20)$$

Although the above is more accurate, it is useful to convert it into a more intuitive form by replacing the denominator on the LHS with $\sigma_{\delta_{\text{TTV}}}$ via analogy to Equation (18). This is somewhat inaccurate because the TTV fit was not a one-parameter fit, and so the real uncertainty may be greater than this due to parameter covariances. Accordingly, the above form is recommended but for the sake of guiding intuition, one may write that

$$\left(\frac{\delta_{\text{TTV}}}{\sigma_{\delta_{\text{TTV}}}}\right) < \left(\frac{\sqrt{3}}{4\pi}\right)\left(\frac{P_P}{T}\right). \quad (21)$$

With the derivation complete, let us take a step back and interpret what has actually been derived. Recall that the inequality imposed is the condition for a plausible moon stemming from Equation (10). How should one interpret the above? Note that the LHS of Equation (21) now represents the TTV signal-to-noise ratio. Therefore, if you have TTV detection with a signal-to-noise of $\gtrsim P_P/(7T)$, then one should expect that derived TDVs will be capable of killing the exomoon hypothesis (assuming they don't see anything). In such cases, if the moon hypothesis is considered viable, it would instructive to derive TDVs then, since their absence would falsify the moon hypothesis.

What if Equation (21) is not satisfied? Is it pointless to derive TDVs? Certainly not. Although one cannot guarantee that the TDVs will be capable of fully excluding the moon hypothesis, they will still place important constraints.

For example, they will still place a minimum constrain on f via Equation (8) - albeit a minimum f which lies within the Hill sphere. This is illustrated in Figure 2 for example (with more specific details about the data provided later in Section 5). This f constraint may still be sufficient to place tension on the moon hypothesis, since only retrograde moons are thought to be dynamically stable beyond $f \gtrsim 0.5$ for example (Domingos et al. 2006). Alternatively, they may actually lead to a TDV detection, thus lending support to the moon hypothesis.

4 THE TTV CEILING

In the previous section, the focus was on the ratio of the TTV amplitude to the upper limit for the TDVs. In some cases, TDV upper limits are not presently available and so it is useful to consider if there is some maximum to how strong the TTV effect of an exomoon can be, in an absolute sense - a TTV ceiling.

The TTV amplitude of an exomoon was first derived in Sartoretti & Schneider (1999) for the case of circular, coplanar orbits. This calculation was generalized to arbitrary orbits in Kipping (2009a), who found that the RMS amplitude is given by

$$\delta_{\text{TTV}} = \left(\frac{1}{2\pi}\right)\left(\frac{a_S M_S P_P}{a_P M_P}\right)\left(\frac{(1-e_S)^2 \sqrt{1-e_P^2}}{1+e_P \sin \omega_P}\right)\left(\sqrt{\frac{\Phi_{\text{TTV}}}{2\pi}}\right). \quad (22)$$

It is first highlighted that the planetary eccentricity terms can be replaced with stellar density observables via the photoeccentric effect (Dawson & Johnson 2012; Kipping et al. 2012), such that:

$$\Psi^{1/3} = \frac{1+e_P \sin \omega_P}{\sqrt{1-e_P^2}} = \left(\frac{\rho_{*,\text{obs}}}{\rho_*}\right)^{1/3}, \quad (23)$$

where ρ_* is the mean density of the host star and $\rho_{*,\text{obs}}$ is the value inferred from a circular orbit fit to the transit light curve. Substituting this into the TTV equation gives

$$\delta_{\text{TTV}} = \left(\frac{1}{2\pi}\right)\left(\frac{a_S M_S P_P}{a_P M_P}\right)\left(\frac{(1-e_S)^2}{\Psi^{1/3}}\right)\left(\sqrt{\frac{\Phi_{\text{TTV}}}{2\pi}}\right). \quad (24)$$

Next, let us use substitute $a_S = fR_{\text{Hill}}$, where $R_{\text{Hill}} \equiv a_P \sqrt[3]{M_P/(3M_*)}$, to give

$$\delta_{\text{TTV}} = \left(\frac{1}{2\pi}\right)\left(\frac{f M_S P_P}{M_P}\right)\left(\frac{M_P}{3M_*}\right)^{1/3}\left(\frac{(1-e_S)^2}{\Psi^{1/3}}\right)\left(\sqrt{\frac{\Phi_{\text{TTV}}}{2\pi}}\right). \quad (25)$$

Let's now proceed to maximize the RHS in order to derive a ceiling for the TTV amplitude. By definition, a moon must satisfy $M_S \leq M_P$ and using this in the above yields the inequality:

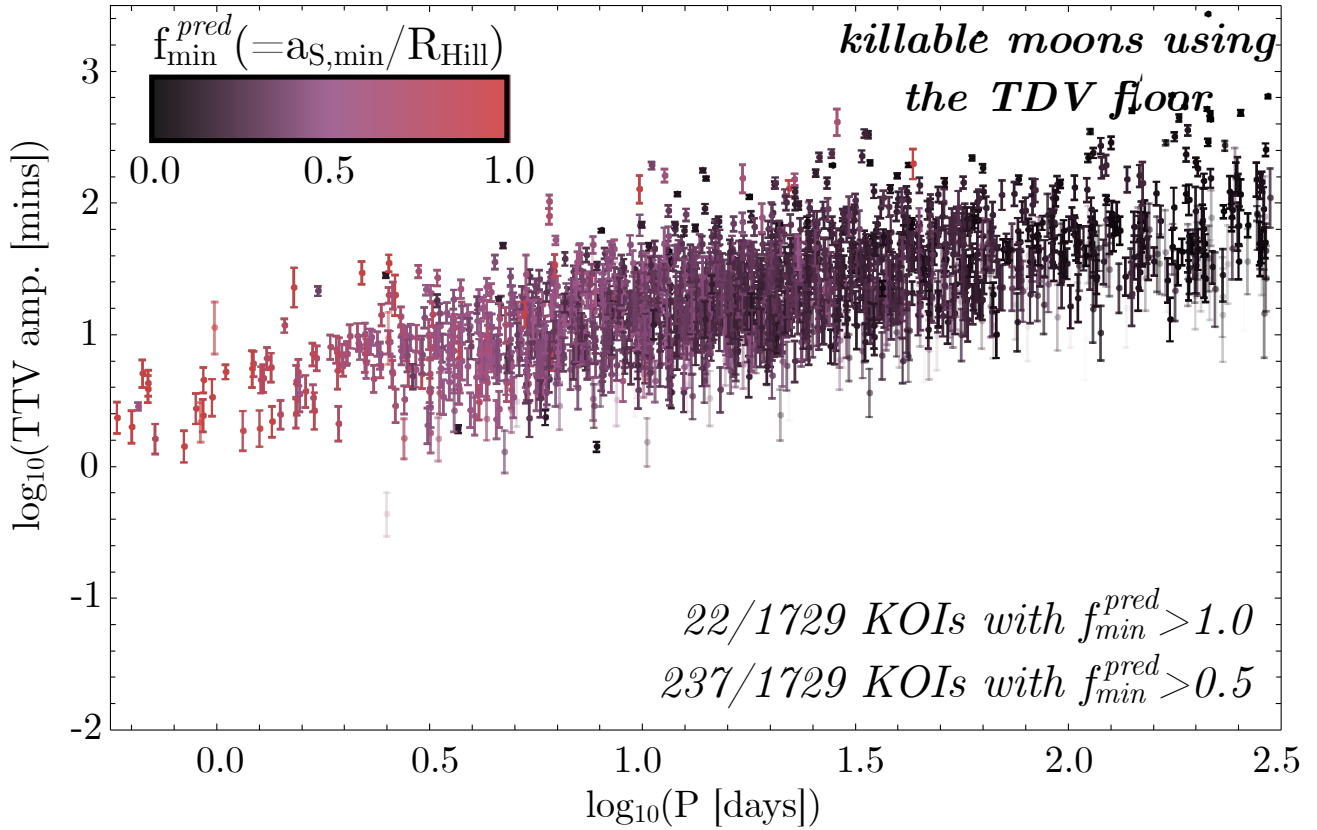


Figure 2. Same as Figure 1 except showing only KOIs for which no TDVs are available. Here, it is assumed that no TDVs will be found and so what is shown is a predicted limit on f using the expected TDV sensitivity from Equation (19) and the minimum f expression of Equation (8). Almost two dozen KOIs with large TTVs are identified that should be “killable” as exomoons, if TDVs were to become available.

$$\delta_{\text{TTV}} \leq f \left(\frac{\Psi^{-1/3}}{n_P} \right) \left(\frac{q}{3} \right)^{1/3} \underbrace{\left((1 - e_S)^2 \sqrt{\frac{\Phi_{\text{TTV}}}{2\pi}} \right)}_{\equiv \beta}, \quad (26)$$

where $q \equiv (M_P/M_*)$ and a new term, β , is defined. It is noted that one could also compute the above with some smaller choice of M_S besides from the the binary limit assumed here, such as one based on a system age plus tidal migration (Barnes & O’Brien 2002). In what follows though, it is preferred to keep the limit as broad as possible to avoid erroneously removing massive moons with unanticipated origins/evolution.

The eccentricity of the satellite is unknown and resides somewhere in the range $0 \leq e_S < 1$ for a stable satellite. Consider the limiting case of $e_S \rightarrow 0$, where Kipping (2011) shows (Equation 6.47) that

$$\lim_{e_S \rightarrow 0} \Phi_{\text{TTV}} = \pi(1 - \cos^2 i_S \sin^2 \varpi_S) \quad (27)$$

The cosine and sine squared terms must always be in the range of zero to unity, and thus

$$0 \leq \left(\lim_{e_S \rightarrow 0} \Phi_{\text{TTV}} \right) \leq \pi \quad (28)$$

which means that

$$0 \leq \lim_{e_S \rightarrow 0} \beta \leq \frac{1}{\sqrt{2}}. \quad (29)$$

Thus, in the limit of circular moons, this term can only ever be smaller than $1/\sqrt{2}$. If one wishes to maximize the RHS of Equation (26) then, one may simply set this combined term to that value. However, this is only true for $e_S \rightarrow 0$ and so let us now consider what the effect of moon eccentricity would be. The $(1 - e_S^2)$ term in front rapidly drops to zero and outpaces the divergent behavior of Φ_{TTV} , causing the combined function to tend to zero as $e_S \rightarrow 1$, which is of course less than $1/\sqrt{2}$. To consider intermediate eccentricities, between 0 and 1, 10^7 Monte Carlo samples were again generated as was done in Section 2 earlier. From this, it was found that the maximum occurs close to (but not exactly) $i_S \rightarrow \pi/2$, $\omega_S \rightarrow \pi/2$ and $\varpi_S \rightarrow 3\pi/2$, for which

$$\lim_{i_S \rightarrow \pi/2} \lim_{\omega_S \rightarrow \pi/2} \lim_{\varpi_S \rightarrow 3\pi/2} \beta = \sqrt{\frac{1 + e_S^2(\sqrt{1 - e_S^2} - 1)}{1 + \sqrt{1 - e_S^2}}}. \quad (30)$$

The RHS is maximized when $e_S = 0.57747\dots$ for which it evaluates to $\beta = 0.71891$. Since this isn’t quite the exact maximum, it was compared to the numerical search which finds the largest ever value of β was 0.719734. Thus, even

with very careful fine tuning, the β term isn't able to noticeably rise above $1/\sqrt{2} = 0.707...$ in value. Setting this as a limit then, Equation (26) becomes

$$\delta_{\text{TTV}} \leq f \left(\frac{\Psi^{-1/3}}{\sqrt{2}n_P} \right) \left(\frac{q}{3} \right)^{1/3} \quad (31)$$

It is now useful to write the amplitude in units of the planetary period, yielding a fractional TTV, and to move the $\sqrt{2}$ next to the RMS amplitude such that it equates to a sinusoid amplitude, yielding

$$\left(\frac{\sqrt{2}\delta_{\text{TTV}}}{P_P} \right) \leq \frac{f}{9} \left(\frac{q}{\Psi} \right)^{1/3}. \quad (32)$$

For planets with Ψ deviating from unity by a large amount, the system would probably be considered suspicious as an exomoon host on the basis that the planet have a high eccentricity (Domingos et al. 2006). Thus, generally, one expects $\Psi \sim 1$, yielding

$$\lim_{e_P \ll 1} \left(\frac{A_{\text{TTV}}}{P_P} \right) < \frac{f q^{1/3}}{9}. \quad (33)$$

The above expression represents a TTV ceiling for exomoons, where a reasonable choice for f would be unity. However, since the TTV amplitude is an observable, one can also re-arrange the above to give another lower limit on f :

$$\lim_{e_P \ll 1} f_{\text{min}} = \left(\frac{9}{q^{1/3}} \right) \left(\frac{A_{\text{TTV}}}{P_P} \right) \quad (34)$$

If an estimate of q is available, it is therefore straightforward to evaluate either of these equivalent expressions. Since q is often not known for transiting planets, it is recommended here that one use an upper limit for the q estimate, so that the above is a conservative evaluation. This is done for the Holczer et al. (2016) KOI sample in Figure 3, with more details provided later in Section 5.

As a more general example, the Jupiter-Sun pair has $q \sim 10^{-3}$ and thus one would not expect fractional TTV amplitudes greater than 1%. For smaller planets, such as the Earth-Sun pair, the maximum allowed fractional TTV amplitude drops another order-of-magnitude to 0.1%. This provides some crude cuts for removing suspiciously large TTV amplitudes in the search for moons.

One might wonder if a TDV ceiling also exists. Recall that the TDVs from an exomoon have two quite distinct components, TDV-V and TDV-TIP. The TDV-V effect is maximized as the moon's semi-major axis tends to zero. Of course, in practice this cannot happen since the moon would impact the planet. However, existing TDV-V theory does not extend to highly compact moons since the derivation of Kipping (2009a,b, 2011) explicitly assume that the moon's velocity is constant during the transit duration. Once the moon's period becomes comparable to the duration or less, this is no longer true.

Further, it is highlighted that the TDV-TIP does not have any true upper limit since it can bob a planet in and out of transit entirely, in principle. Thus, one would obtain

a series of missed transits within the overall sequence. For these reasons, combined with the fact any kind of TDV detection is relatively rare, no effort was made to deduce a TDV ceiling here.

5 APPLICATION

5.1 Applying to the Holczer et al. (2016) Catalog

To apply these formulae, one requires a homogeneous catalog of both TTVs and TDVs for a sample of transiting planets. To this end, the Holczer et al. (2016) catalog is utilized, which includes TTVs for 2599 *Kepler* Objects of Interest (KOIs). It was decided to perform an independent analysis of these TTVs, in order to measure putative TTV amplitudes for each, the statistical significance of said signals, and upper limits on the TDVs. The catalog includes TTVs for all 2599 KOIs and TDVs for cases where the authors deemed the data quality was sufficient to attempt their derivation.

First, for each KOI, the dispersion of the TTVs is recorded by measuring the scatter of the TTV measurements divided by their uncertainties. This essentially tracks how many “sigmas” the TTV points are dispersed about zero. To account for possible outliers, the median deviation multiplied by 1.4286 is used as our measure of scatter. Any TTV measurements which exhibit a deviation from zero greater than 10 times this value are then removed. A further cull is applied to any TTV measurements where the TTV uncertainty is more than 3 times greater than the median TTV uncertainty. The same process is applied to the TDVs, where available.

Next, a Lomb-Scargle (LS) periodogram (Lomb 1976; Scargle 1982) is run through the TTVs using a log-uniformly spaced grid of periods from the Nyquist period out to twice the baseline of observations. The log-period spacing of this grid was set to $\log_2(0.01)$. At each period, the best fitting sinusoid is computed using a weighted linear least squares regression, saving the χ^2 of the fit and the amplitude. Once the periodogram is complete, the peak of highest χ^2 improvement over a flat line is saved, whose period, amplitude and χ^2 are used in what follows. These TTV amplitudes comprise the y-axis information of Figures 1, 2 & 3, where the TTV amplitude uncertainty is assigned using Equation (18) - but with the “TDV” subscripts replaced with “TTV”.

Next, a filter is applied to only accept KOIs for which the best sinusoidal fit is statistically favoured over a simple flat line. This is accomplished by calculating the Bayesian Information Criterion (BIC) difference between the two models (Schwarz 1978), and selecting only KOIs where the sinusoid yields an improved BIC. From this, it was found that the vast majority, 2437 of the 2599 KOIs, favor the sinusoidal TTV model. Indeed, 1810 of these would be classed as “very strong” ($\Delta\text{BIC} > 10$) using the Kass & Raftery (1995) interpretative scale. This highlights just how valuable tools to quickly classify this large number of detections can be. The TTV amplitudes and ΔBIC scores for each of 2437 KOIs are listed in Table 1.

For the TDVs, one can first exploit the fact that the hypothesis that is being tested requires the TDV period to be equal to the TTV period (Kipping 2009a,b). One can therefore simply fix the TDV period to that resulting from

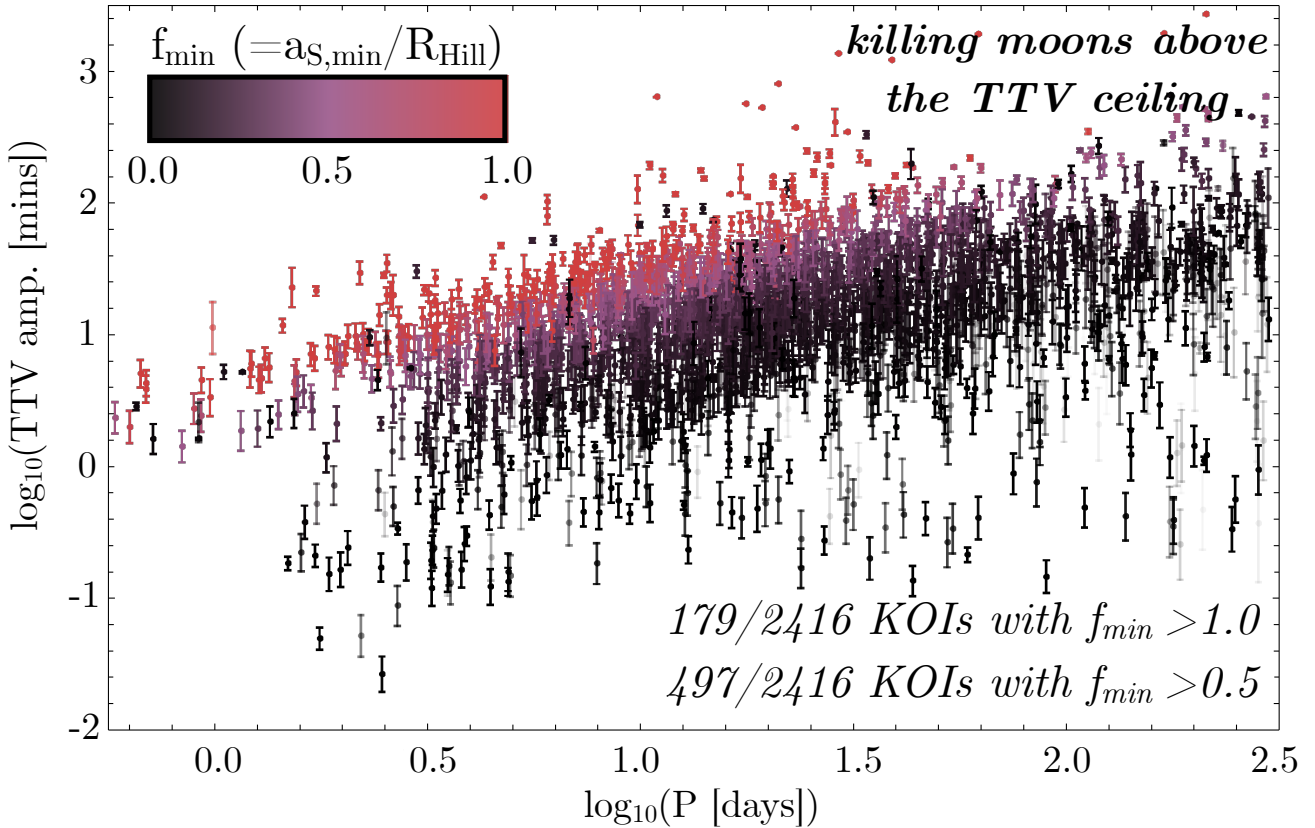


Figure 3. Same as Figure 1 except the minimum exomoon semi-major axis (normalized by the planetary Hill radius) is calculated using the TTV ceiling effect of Equation (34). On this basis, 179 KOIs can be rejected as being plausibly due to a single exomoon, shown in red. Note that all 2437 KOIs are not shown from the full sample, since 21 do not have planetary radii necessary to compute the TTV ceiling and are thus removed.

the earlier TTV periodogram. It also noted TDVs due to an exomoon are generally expected to be dominated by TDVs (Kipping 2009b) with a phase-lag of $\pi/2$ radians. This reduces the TDV fit to a single parameter; amplitude. This also makes the estimate of TDV error and 3σ upper limit straight-forward, since for a one-parameter model such as this one can simply use $\Delta\chi^2$ to extract errors.

After running through all KOIs, only two KOIs were found with a strong preference for a coupled TDV signal ($\Delta\text{BIC} > 10$), KOI-1546.01 and KOI-5802.01, which may deserve further attention. For the others, the TDV 3σ upper limit is used to compute f_{\min} via Equation (8), where basic transit parameters (e.g. transit duration) are taken from the NASA Exoplanet Archive (Akeson et al. 2013). From this, Figure 1 is produced, which identifies 40 “impossible moons” from 708 KOIs with TDVs. If the constraint is tightened such that only prograde moons are permitted ($f < 0.5$), then this substantially increases to 198 KOIs.

In cases without any available TDVs, it is instead investigated what constraint on f_{\min} one might expect them to provide, if they were to be derived. This is done following the methods described in Section 3, where it is assumed that no TDVs will be found and calculate a predicted limit on f using expected TDV sensitivity from Equation (19) and the minimum f expression of Equation (8). Figure 2 shows the result of this exercise, where identify 20 KOIs (out of

1729 without TDVs) for which TDVs measurements should be able to completely exclude the exomoon hypothesis, assuming no TDVs are found. Again, this steeply rises to 237 if one allows prograde moons only.

The accuracy of the predicted f_{\min} values can be tested applying the same procedure to the 708 KOIs in the full sample which truly do have TDVs. In this way, one can plot the predicted f_{\min} against the calculated f_{\min} values found earlier. This is shown in Figure 4, where a nearly 1:1 relation is obtained, as expected. From the figure, one can see subset of KOIs for which the predicted f_{\min} are too optimistic, which is to be expected since the real duration measurements can be occasionally degraded in precision due to effects such as data gaps, star spots and flaring.

Finally, for the TTV ceiling, one needs an estimate of q mass ratio between the planet and the star. For this, the Chen & Kipping (2017) mass-radius relation is used in what follows. In cases where the relation becomes degenerate (specifically around a Jupiter radius), the upper allowed limit on the mass is used, following the argument outlined earlier in Section 4. For 21 KOIs, the NEA does not list a planetary radius (or transit depth) and thus it was not possible to estimate a TTV ceiling for these cases³.

³ These are KOIs 2311.01, 2640.01, 4956.01, 5000.01, 5074.01, 5160.01, 5161.01, 5177.01, 5194.01, 5210.01, 5309.01, 5368.01,

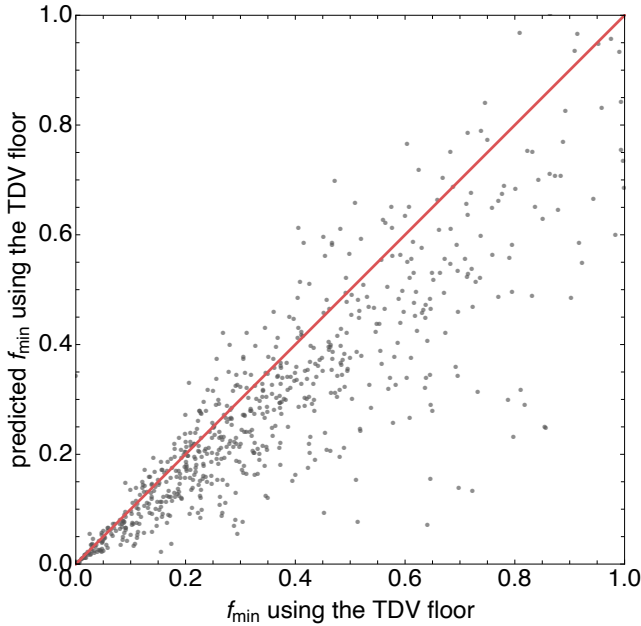


Figure 4. Comparison of the predicted lower limits on f versus the actual obtained values for 708 KOIs. It was found that the predictions are generally sound, although there is some subset of KOIs for which the real TDV precision is worse than the forecasted value.

The TTV ceiling criterion provides the greatest number of impossible moons, 179 KOIs. These consistently show the highest TTVs for planets of comparable periods; the upper tail of the TTV amplitude distribution. These are surely interesting TTV systems, being highly significant, but can be rejected for an exomoon survey. These f_{\min} limits are made available in Table 1.

5.2 Application to Kepler-1625b

Additionally, the methods described in this work are applied to the only known example of an exomoon candidate - Kepler-1625b i (Teachey & Kipping 2018).

Since no TDVs were explicitly derived in the original paper, it is first necessary to obtain them. A starting point for this process are the transit fits and processed data used by Teachey & Kipping (2018). In particular, the “T” model of that work is a suitable jumping off point, which assumes that no moon is present and just fits the light curve trends and transit profile with a simple Mandel & Agol (2002) model. The “T” stands for TTVs, because the model gives each epoch its own transit time as a free parameter, but the other parameters, such as impact parameter and stellar density, are globally shared across all epochs (which imposes a constant duration). Starting from this model, it is updated to let ρ_* also be uniquely assigned to each epoch. This increases the dimensionality of the “T” model by three new parameters (four epochs minus the original global stellar density

term). Since the stellar density controls the planetary semi-major axis, which in turn controls the planetary velocity, this inclusion allows for the measurement of the TDV-Vs directly.

For the models that do not include a moon, the agreement between the different trend models attempted by Teachey & Kipping (2018) are excellent and on this basis the exponential long-term trend model is adopted in what follows.

With this new TDV model, the four light curves provided by Teachey & Kipping (2018) are re-fit using MULTINEST (Feroz & Hobson 2008; Feroz et al. 2009), yielding a chronological sequence of durations (using definition \tilde{T} ; Kipping 2010) of 1039^{+18}_{-17} mins, 1068^{+16}_{-14} mins, 1034^{+26}_{-68} mins and $1063.7^{+6.2}_{-5.4}$ mins. The most recent duration here comes from the HST observations of Teachey & Kipping (2018), which clearly provides substantial improvement in precision.

The constant duration model performs well against these data, with $\chi^2 = 2.967$ for four data points. As an additional check on this, one may compare the Bayesian evidences between the original “T” model of Teachey & Kipping (2018) and this modified model which allows for TDVs. From this, it is found that the original model is indeed favoured with a Bayes factor of $K = 87,000$ - a decisive preference for a constant duration model. Accordingly, it is concluded that there exists no evidence for detectable TDVs. This is perhaps not surprising given that the Teachey & Kipping (2018) solution places the moon at a fairly wide separation, where TDVs are attenuated.

Having established that no TDVs exist, the next step is to calculate an upper limit on the TDV amplitude. This is straight-forwardly achieved by fitting an offset + sinusoid to the derived durations using a simple MCMC, infers a 3σ upper limit on the TDV amplitude of 55 mins.

It is now possible to use the TDV upper limit along with the TTV amplitude to infer the minimum allowed exomoon semi-major axis, without ever formally fitting the data to an exomoon model. The TTV amplitude is not actually fit per say in Teachey & Kipping (2018), but rather is incorporated into their photodynamical planet+moon solution. From the reported TTVs, a sinusoid was regressed to obtain $A_{\text{TTV}} = (19.1 \pm 1.9)$ minutes. The ratio of the quoted uncertainty compared to the amplitude indicates that this is highly significant and indeed this has already been established through the Bayes factor comparison in Teachey & Kipping (2018), who find a $K = 10.0$ in favor of the TTV model over a static case. Plugging these numbers into Equation (8) yields $f > 0.046$.

For the TTV ceiling effect, a rough estimate can be found by simply assuming the planet is of order of a Jupiter mass, given that it approximately a Jupiter radius. Using Equation (34), this yields $f > 0.0042$. Thus, in this case, the TDV floor limit imposes a tighter constraint. Certainly then, there is plenty of room for an exomoon given the current timing measurements. Indeed, the exomoon solution of Teachey & Kipping (2018) places the moon at $f \simeq 0.2$, which satisfies this minimum constraint.

5374.01, 5377.01, 5437.01, 5450.01, 5537.01, 5783.01, 5824.01, 5837.01, 5955.01.

Table 1. Results from our application of the methods described in this work to the transit timing catalog of the KOIs presented by [Holczer et al. \(2016\)](#). Only a portion of the table is shown here.

KOI	P [d]	A_{TTV} [m]	$\Delta(\text{BIC})_{\text{TTV}}$	f_{\min} (TDV)	f_{\min}^{pred} (TDV)	f_{\min} (TTV)	TDVs?
1.01	2.471	0.0265 ± 0.0082	8.4	0.874	0.707	0.000154	✓
2.01	2.205	0.052 ± 0.019	2.8	1.44	1.45	0.000386	✓
3.01	4.888	0.133 ± 0.033	23.5	0.638	0.472	0.00404	✓
....

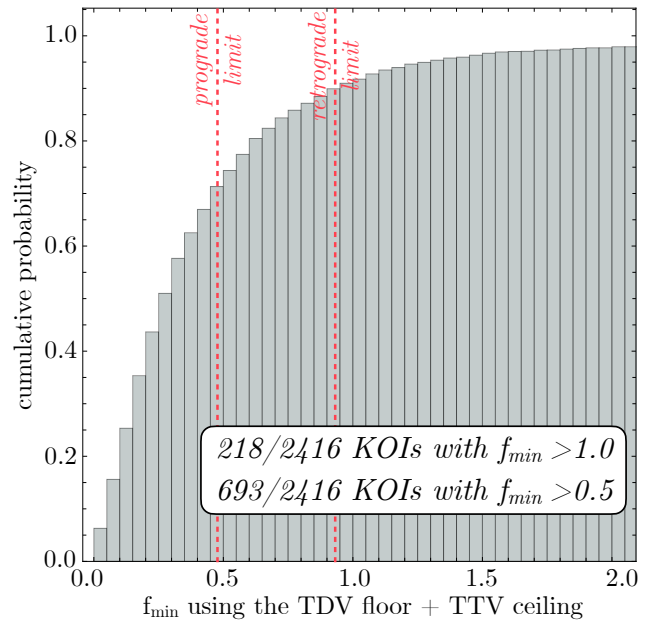
6 DISCUSSION

This work derives two distinct, but related, means of calculating a lower limit on an exomoon’s semi-major axis divided by its planetary Hill radius, conditioned upon the hypothesis that an observed (and significant) TTV is solely caused by a single exomoon. If either of these lower limits exceeds unity (i.e. the moon is outside the Hill sphere), the hypothesis can be rejected on the via an argument of *reductio ad absurdum*. One is free to modify the critical limit to less than unity, under more conservative assumptions regarding the range of stable moons (e.g. see [Domingos et al. 2006](#)).

The two methods both assume that a TTV detection has been made and that one has in hand a TTV amplitude. They differ in whether they assume an upper limit on the TDV amplitude has been computed. Most directly, our work asks whether the detected TTV amplitude could plausibly be caused by an exomoon? Of course, if a signal passes these tests, that does not mean that one can necessarily claim an exomoon detection on this basis alone. However, failing one of the criteria is damning for the hypothesis that the observed TTVs are solely caused by a single exomoon. Nevertheless, one could suggest that some component of the TTVs are still caused by one (or more) moons, with other TTVs effects contributing to the total - although the additional complexity of such a hypothesis would certainly necessitate some specific motivation to justify.

The two limits are given by Equations (8) & (34). Since both require the TTV amplitude, but only the former requires the TDV upper limit, it is worthwhile pausing to ask whether the former ever realistically undercuts the latter, or can we generally rely on Equation (34) alone for the best limits? From the applied examples in this work, using the [Holczer et al. \(2016\)](#) *Kepler* transit timing catalog, 40 impossible moons were identified via Equation (8), and 179 via Equation (34), but critically only one object which appears in both lists (KOI-5497.01). Tightening the f constraint to only prograde moons ($f < 0.5$) yields many more impossible moons for both methods (see Figures 1 & 3) yet only one new overlapping object (KOI-4927.01). It is further highlighted that the TTV ceiling requires an estimate of the planet-to-star mass ratio, whereas the TDV floor does not. Thus, the two limits are highly complementary and the use of both is recommended.

This work highlights that there are a considerable number of KOIs for which TDVs would be useful. Of the 1709 KOIs without TDVs in the used sample, it was found that 22 should be expected to yield a TDV upper limit sufficient to completely exclude moons (since $f_{\min} > 1$). Of these 22, 11 already have a TTV ceiling constraint that indicates

**Figure 5.** Cumulative histogram of the f_{\min} value derived using both the TDV floor and TTV ceiling together (taking the maximum of the two) for the KOIs in our sample. About 9% of the sample can be rejected as being plausibly due to an exomoon using the most generous assumptions about moon stability ($f < 1$), and 29% using $f < 0.5$.

an impossible moon. For the other 11 (KOIs 72.01, 452.01, 732.01, 1300.01, 1428.01, 2215.01, 2573.01, 3913.01, 4927.01, 5128.01, 5713.01), the current TTV constraints do not fully prohibit an exomoon and thus these would make interesting objects for follow-up investigations.

Repeating this for a critical f threshold of 0.5 increases the number of KOIs deserving of TDV follow-up to 109 - Table 1 provides a full list of these. A cumulative histogram of the best possible constraint on f is shown Figure 5 for the full sample used in this work.

It is briefly highlighted that application of these techniques to *Kepler*-1625b offers another example of a test that this moon candidate survives. As emphasized earlier, passing this test does not itself prove the case for a moon, but failure to do would have provided a simple means to discard the exomoon candidate.

As demonstrated from these examples, the tests discussed here provide a simple and well-motivated test to remove spurious signals in the search for exomoons. Their application is encouraged to those looking for such effects, as an

expedient means of removing false-positives. More broadly, this work showcases the value of timing effects and the benefits of community derived TTVs and TDVs.

ACKNOWLEDGMENTS

DK is supported by the Alfred P. Sloan Foundation. AT is supported through the NSF Graduate Research Fellowship (DGE-1644869). Thanks to Dan Fabrycky for helpful comments on a preliminary draft. This work is based in part on observations made with the NASA/ESA Hubble Space Telescope, obtained at the Space Telescope Science Institute, which is operated by the Association of Universities for Research in Astronomy, Inc., under NASA contract NAS 5-26555. These observations are associated with program #GO-15149. Support for program #GO-15149 was provided by NASA through a grant from the Space Telescope Science Institute, which is operated by the Association of Universities for Research in Astronomy, Inc., under NASA contract NAS 5-26555. This paper includes data collected by the Kepler mission. Funding for the Kepler mission is provided by the NASA Science Mission directorate. This research has made use of the NASA Exoplanet Archive, which is operated by the California Institute of Technology, under contract with the National Aeronautics and Space Administration under the Exoplanet Exploration Program.

REFERENCES

- Agol, E., Steffen, J., Sari, R., Clarkson, W., 2005, MNRAS, 359, 567
- Akeson, R. L., Chen, X., Ciardi, D., et al., 2013, PASP, 125, 989
- Ballard, S., Fabrycky, D., Fressin, F., et al., 2011, ApJ, 743, 200
- Barnes, J. W. & O’Brien, D. P., 2002, ApJ, 575, 1087
- Carter, J. A., Yee, J. C., Eastman, J., Gaudi, S. B., Winn, J. N., 2008, ApJ, 689, 499
- Chen, J. & Kipping, D., 2017, ApJ, 834, 17
- Dawson, R. I. & Johnson, J. A., 2012, ApJ, 756, 122
- Deck, K. M. & Agol, E. M., 2016, ApJ, 821, 96
- Díaz, R. F., Rojo, P., Melita, M., Hoyer, S., Minniti, D., Mauas, P. J. D., Ruíz, M. T., 2008, ApJL, 682, L49
- Dobrovolskis, A. R. & Borucki, W. J., 1996a, Influence of Jovian Extrasolar Planets on Transits of Inner Planets. In: AAS/Division for Planetary Sciences Meeting Abstracts #28, Bulletin of the American Astronomical Society, vol 28, p 1112
- Dobrovolskis, A. R. & Borucki, W. J., 1996b, Influence of Jovian extrasolar planets on transits of inner planets. In: Bulletin of the American Astronomical Society, BAAS, vol 28, p 1112
- Domingos, R. C., Winter, O. C., Yokoyama, T., 2006, MNRAS, 373, 1227
- Feroz, F. & Hobson, M. P., 2008, MNRAS, 384, 449
- Feroz, F., Hobson, M. P. & Bridges, M., 2009, MNRAS, 398, 1601
- Hadden, S. & Lithwick, Y., 2014, ApJ, 787, 80
- Hadden, S. & Lithwick, Y., 2017, AJ, 154, 5
- Holczer, T., Mazeh, T., Nachmani, G., et al., 2016, ApJS, 225, 9
- Holman M. J., Murray, N. W., 2005, Science, 307, 1288
- Holman M. J., Fabrycky, D. C., Ragozzine, D., et al., 2010, Science, 330, 51
- Hrudková, M., Skillen, I., Benn, C. R., et al., 2010, MNRAS, 403, 2111
- Kass, R. E. & Raftery, A. E., 1995, 90, 773
- Kipping, D. M., 2009a, MNRAS, 392, 181
- Kipping, D. M., 2009a, MNRAS, 392, 181
- Kipping, D. M., 2009b, MNRAS, 396, 1797
- Kipping, D. M., 2010, MNRAS, 407, 301
- Kipping, D. M., 2011, Ph.D. thesis, University College London, arXiv e-prints:1105.3189
- Kipping, D. M., Dunn, W. R., Jasinski, J. M., Manthri, V. P., 2012, MNRAS, 421, 1166
- Lithwick, Y., Xie, J., Wu, Y., 2012, ApJ, 761, 122
- Lomb, N. R., 1976, Ap&SS, 39, 447
- Maciejewski, G., Dimitrov, D., Neuhäuser, R., Niedzielski, A., Raetz, St., Ginski, Ch., Adam, Ch., Marka, C., Moualla, M., Mugrauer, M., 2010, MNRAS, 407, 2625
- Mandel, K. & Agol, E., 2002, ApJ, 580, 171
- Miller-Ricci, E., Rowe, J. F., Sasselov, D., et al., 2008a, ApJ, 682, 586
- Miller-Ricci, E., Rowe, J. F., Sasselov, D., et al., 2008b, ApJ, 682, 593
- Miralda-Escudé, J., 2002, ApJ, 564, 1019
- Nesvorný, D. & Morbidelli, A., 2008, ApJ, 688, 636
- Nesvorný, D. & Beaugé, C., 2010, ApJ, 709, 44
- Nesvorný, D., Kipping, D., Terrell, D., Hartman, J., Bakos, G. Á., Buchhave, L. A., 2013, ApJ, 777, 3
- Nesvorný, D. & Vokrouhlický, D., 2014, ApJ 790, 58.
- Rabus, M., Deeg, H. J., Alonso, R., Belmonte, J. A., Almenara, J. M., 2009, MNRAS, A&A, 508, 1011
- Ribas, I., Font-Ribera, A., Beaulieu, J., Morales, J. C., & García-Melendo, E. 2009, in IAU Symp., 253, 149
- Sartoretti, P. & Schneider, J., 1999, A&AS, 14, 550
- Scargle, J. D., 1982, ApJ, 263, 835
- Schneider, J., 2003, Multi-planet system detection by transits. In: Combes F, Barret D, Contini T Pagani L (eds) SF2A-2003: Semaine de l’Astrophysique Française, p 149
- Schneider, J., 2004, Multi-planet system detection with Eddington. In: Favata F, Aigrain S Wilson A (eds) Stellar Structure and Habitable Planet Finding, ESA Special Publication, vol 538, pp 407–410
- Schwarz, G., 1978, Annals of Statistics, 6, 461
- Steffen, J. H. & Agol, E., 2005, MNRAS, 364, L96
- Szabó, Gy. M., Szatmáry, K., Divéki, Zs., Simon, A., 2006, A&A, 450, 395
- Simon, A., Szatmáry, K., Szabó, Gy. M., 2007, A&A, 470, 727
- Szabó, Gy. M., Pál, A., Derekas, A., Simon, A. E., Szalai, T., Kiss, L. L., 2012, MNRAS, 421, L122
- Teachey, A., Kipping, D., Schmitt, A. R., 2018, AJ, 155, 36
- Teachey, A. & Kipping, D., 2018, Science Advances, 4, 1784
- Wu, Y. & Lithwick, Y., 2013, ApJ, 772, 74

This paper has been typeset from a \LaTeX file prepared by the author.